Texture-based Image Retrieval Based on FABEMD

M. H. Ould Mohamed Dyla, H.Tairi

Faculty of Sciences Dhar El Mahraz
BP 1796 FES Morocco

Abstract

In this paper, we present a new method for content based images retrieval (CBIR). We propose characterizing images by using global information extracted from the Fast and Adaptive Bidimensional Empirical Mode Decomposition (FAEMD), which decomposes image into a set of functions named Bidimensional Intrinsic Mode Functions (BIMF) and a residue. On the first two BIMFs, which contains a high frequency part of the image, eventually curves and edges, Curvelet transform (CT) was applied; wheras on the remaining part of the image Gabor wavelets (GW) were applied. Image feature based on Curvelet transform and Gabor wavelet, are then calculated. Our approach was tested on Brodatz database. Experimental results show that the proposed system outperforms previous rotation-invariant systems significantly, and it is found to be superior to Curvelet Transform and Gabor wavelets.

Keywords: Content Based Image Retrieval, FABEMD, Curvelet Transform, Gabor Wavelets.

1. Introduction

Content based image retrieval (CBIR) systems have been one of the most active areas of research in computer science. It remains an active area of research today due to its applications in various fields like commerce, government, academia, and hospitals. Therefore, many image retrieval systems such as QBIC, MARS, Virage, FIDS, Photobook, WebSEEk, etc. have been built. The CBIR systems can be classified broadly into two categories: Low level feature based system and High level or Semantic feature based system. Low level features are general features and computed from pixel values. However, high level features are abstract attributes involving a significant amount of reasoning. Our work falls into the first category.

Feature extraction is one of the most important tasks for efficient and accurate image retrieval purpose. Shape, texture and color are three main groups of features that are being used in CBIR systems. Shape is represented by circularity, eccentricity, Fourier descriptor [1], moment invariants [2], histogram of values after applying Sobel edge filter [3], edge layout vector [4], shape context descriptor [5] , etc. A variety of techniques have been used for measuring texture such as co-occurrence matrix [6], Gabor filter [7] and fractals [8].

Texture is an important property of digital images. A successful CBIR system must be able to deal with textured images in practical application. Several models have been proposed to analyze textures, such as grey-level co-occurrence matrices, Markov random field model [9], and simultaneous auto-regressive model [10], and World decomposition model [11]. Most of spatial domain texture analysis models have a fundamental weakness that the image is analyzed at a single scale. This aspect can be improved with a joint spatial frequency multi-channel representation methodology, usually a joint spatial frequency multi-channel.

Representation methodology is used to deal with scale changes involved in textured image. However, this leads often to a relative efficiency according to the complexity and wealth information which contains the considered image database. Alternative methods of texture analysis for image retrieval include the use of Gabor filters [7], Wavelet [12] and DCT [13]. However, most of them are not able to accurately capture the edge information which is the most important texture feature in an image.

The wavelets (DWT), have had a huge success in the field of image processing, and have been used for many problems such as compression, image restoration, image retrieval, etc. However, it is now clear that the wavelets are not optimal for the analysis of anisotropic objects in the image (lines, contours ...), but still effective in the detection of isotropic structures at different scales.

Then, Wavelet transform cannot represent objects containing randomly oriented edges and curves as it is not good at representing line singularities. Gabor filters are found to perform better than wavelet transform in representing textures and retrieving images due to its multiple orientation approach [7]. However, due to the loss of spectral information in Gabor filters, they cannot effectively represent images. This affects the CBIR performance. Consequently, a more robust mechanism is necessary to improve CBIR performance. To achieve a complete coverage of the spectral domain and to capture more orientation information, Curvelet transform has been developed. It captures edge information or texture

information more accurately than Wavelet and Gabor filters [14, 15].
In this paper we propose a realistic improvement which is performed under a convenient decomposition of the image. Our approach is based on the Fast and Adaptive Bidimensional Empirical Mode Decomposition (FABEMD) [16], which decomposes image into a set of functions named Bidimensional Intrinsic Mode Functions (BIMF) and a residue. on the first two BIMFs, which contains a high frequency part of the image, eventually curves and edges, Curvelet transform was applied; whereas on the remaining part of the image Gabor filters were applied; then the low order statistic from the transformed images was counted. A quantitative comparison showed a significant improvement in the presence of decomposition and an appropriate weighted similarity measure allows to converge toward a better results.

The structure of this paper is as follows. Section 2 describes the way in which the efficient matching of features between a query image and an images database is achieved. Section 3 describes an experiment study. Section 4 concludes the paper.

2. Proposed Approach

Textured Images Databases Systems are radically different from conventional information systems. Many new issues need to be addressed. The system should be able of providing access to the content of images. Our approach to build a CBIR system approach is conceptually described by the framework depicted in figure 1. The core of the system is a new retrieval system based on the information derived from an image decomposition procedure. The database will be structured in an identical fashion, in such a way to allow us to access the information in a same format which can be easily compared.

In the context of textured databases, this study presents a new approach where we first proceed to a decomposition of the query image into two components using the Fast and Adaptive Bidimensional Empirical Mode Decomposition (FABEMD). The features extraction is not applied directly on the query image but after doing a decomposition scheme. Sections 2.1 explain the decomposition model of image, while the section 2.2 defines feature extraction of vector descriptor.

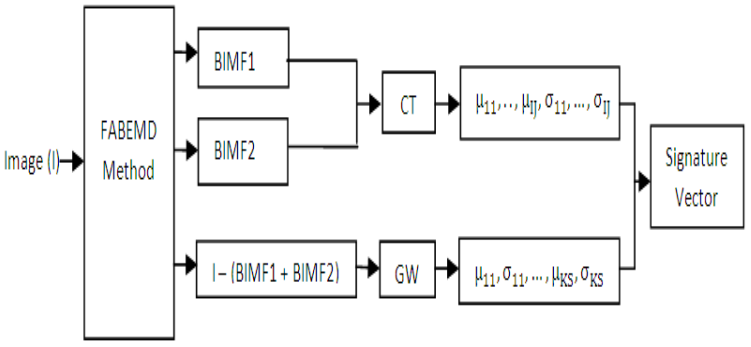

Fig. 1: Extraction of image signature

2.1 Fast and adaptive Bidimensional Empirical Mode Decomposition (FABEMD).

The EMD method is an adaptive decomposition which was first introduced by Huang and al [17]. This method is appropriate for non linear, non stationary signal analysis. The concept of EMD is to decompose the signal into a set of zero mean functions called Intrinsic Mode Functions (IMF) and a residue. As the increasing of decomposition level, the IMF decreases. Huang et al. defined IMF as function that satisfies two conditions: a) the numbers of extrema and zero-crossings are either equal or differ by at most one; b) the mean value of the envelopes defined by the local maxima and minima is zero at every point.

Given a signal S(t), the sifting process of EMD can be summarized as follows :

1) Identify all local extrema of S(t).
2) Interpolate all local maxima to get upper-envelope $e_{max}(t)$ and all local minima to get lower-envelope $e_{min}(t)$.
3) Compute the local mean : $m(t) = \frac{e_{max}(t) + e_{min}(t)}{2}$
4) Compute $d(t) = S(t) - m(t)$. $d(t)$ is the candidate to be an IMF.
5) If $d(t)$ satisfies the definition of IMF, subtract it from the signal $r(t) = S(t) - d(t)$ and go to step 6. If $d(t)$ does not satisfy the definition of IMF, go to step 1 and use $d(t)$ instead of $S(t)$.

Steps 1-5 are repeated until $d(t)$ satisfies the definition of IMF.

6) If $r(t)$ residue is a monotone function, the decomposition process is complete.

If residue $r(t)$ is not a monotone function, go to step 1 and use $r(t)$ instead of $S(t)$.

The process of getting each IMF (steps 1-4) is called sifting process. When the decomposition is complete, the original signal s(t) can be represented like this:

$$S(t) = \sum_{k=1}^{N} IMF_K + r(t) \quad (1)$$

Following Nunes and al. [18], Bidimensional Empirical Mode Decomposition (BEMD) is defined as follows:

- Identify the extrema (maxima and minima) of the image I.
- Generate the 2D 'envelope' by connecting maxima points (respectively, minima points) with 2D interploation methods.
- Averaging the two envelopes to compute the local mean m.
- Since BIMF should have zero local mean, subtract out the mean from the image: $h = I - m$.
- repeat until h is BIMF.

However, Extraction of each IMF requires several iterations. Because the surface interpolation method itself fits a surface in an iterative optimization approach, it makes the BEMD process complex and excessively time consuming. Effects of incorrect interpolation due to the lack of extrema points at the boundary region and very few arbitrarily distributed extrema points at some stages of the process impose severe restriction on the application of BEMD. Although a few modifications have been suggested in the literature to improve the process [18-19], BEMD still suffers from the above mentioned problems to some extent.

In 2008, Bhuiyan and al. [16] introduced a new approach to make BEMD fast and adaptive (FABEMD). FABEMD enables the decomposition of images with any dimensions in a very short period of time.

FABEMD differs from the original BEMD algorithm, basically in the process of estimating the upper and lower envelopes (FABEMD replaces the interpolation step by a direct envelope estimation method) and in limiting the number of iterations per BIMF to one. To summarize, the upper and lower envelope formation in FABEMD requires three steps: window size determination, getting the MAX (MIN) filter output and averaging smoothing, all these operations can be done very fast using efficient programming routines.

In [16] a comparative study between BEMD and FABEMD is presented in detail, and showed that FABEMD ensures a more accurate estimation of the BIMFs than BEMD. In figure 2, we give an example of FABEMD decomposition for a image.

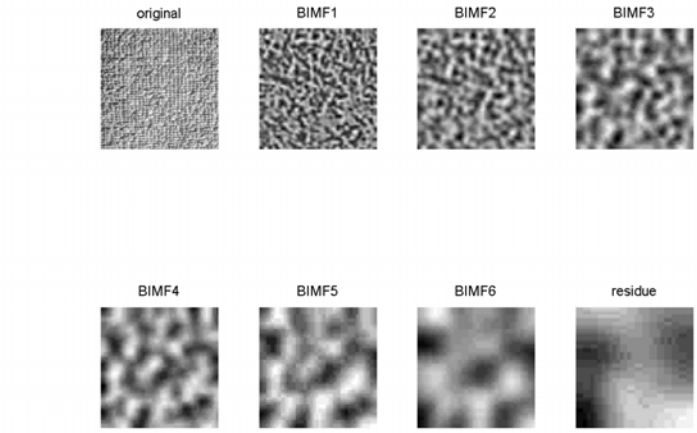

Fig. 2. Decomposition obtained by FABEMD.

In [21], the author uses the FABEMD for generating CBIR images signatures. In his experience, he decomposes the image into six BIMFs and then applying the generalized Gaussian on each one. However, the decomposition of image into six BIMFs is not always possible because some images can be decomposed only to a number less than six BIMFs. Moreover, by applying the same procedure (generalized Gaussian), the author has not considered the fact that BIMFs are different.

In our approach, we decompose the image by FABEMD into two components: the first component contains the sum of the two first BIMFs, and the second component contains the remaining part of the image.

Since the first BIMFs contains the highest local frequencies of oscillation or the highest local spatial scales the first component contains the edges and the curves of image. We apply, therefore, the Curvelet transform, which is optimal for the analysis of anisotropic objects in image (e.g., curves, edges). On the second component, we apply the Gabor wavelets which still effective for the detection of isotropic structures at different scales.

In our approach, we also reduce the computational time by decomposing the image only into two components. We give in table 1, the computing time to decompose an image with different size, using FABEMD.

Table 1. Compute time to decompose an image by FABEMD.

Image size	*128*128*	*512*512*
FABEMD on 6 FABIMF	2.23 s	49 s
FABEMD on 2 FABIMF	0.68 s	14 s

2.2 Feature extraction

2.2.1 Description of Curvelet Transform

Initially, the concept and implementation of Curvelet transform comes from Ridgelet transform, which is a specified kind of wavelets with the directions along edges and perpendicular to edges. Therefore, let's start from the definition of ridgelet transform. Given an image function f(x,y) the continuous ridgelet transform is given as :

$$\Re_f(a,b,\theta) = \iint \psi(x,y)f(x,y)dxdy \quad (2)$$

where a>0 is the scale, $b \in R$ is the translation and $\theta \in [0,2\pi)$ is the orientation. The ridgelet is defined as :

$$\psi_{a,b,\theta}(x,y) = a^{-\frac{1}{2}}\psi\left(\frac{x\cos(\theta)+y\sin(\theta)-b}{a}\right) \quad (3)$$

Figure 3 shows a typical ridgelet [15]. It is oriented at an angle θ, and is constant along lines: $x\cos(\theta)+y\sin(\theta)=\text{const}$. It can be seen that a ridgelet is linear in edge direction and is much sharper than a conventional sinusoid wavelet.

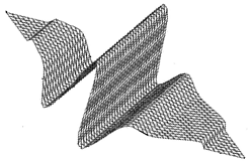

Fig. 3 : A ridgelet Waveform

This similarity means that like Gabor, a ridgelet can be tuned at different scales and orientation to create Curvelets. But different from Gabor filters which only cover part of the spectrum in the frequency domain [7], Curvelets have a complete cover of the spectrum in frequency domain. That means, there is no loss of information in Curvelet transform in terms of capturing the frequency information from images.

Figure 4 shows the Curvelet tiling and cover of the spectrum of a 512x512 images with 5 scales [22]. The shaded wedge shows the frequency response of a Curvelet at orientation 4 and scale 4. It can be seen, the spectrum cover by Curvelets is complete. In contrast, there are many holes in the frequency plan of Gabor filters Figure 5.

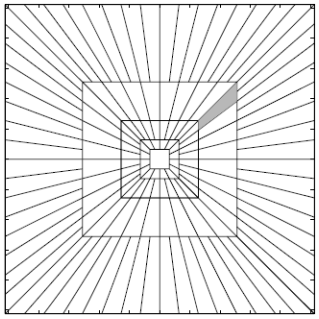

Fig. 4: the tiling of frequency plan by Curvelets

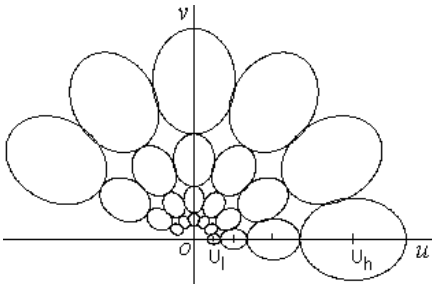

Fig. 5 : The tiling of half frequency pan by Gabor filters

2.2.2 Gabor wavelets

Wavelet theory is a unified and effective mathematical framework for multichannel image analysis [23]. In particular, Gabor functions have been extensively studied for texture discrimination, texture segmentation and image retrieval, etc. and have been shown to be very efficient. In [7], it has shown that image retrieval using Gabor features outperforms that using pyramid structured wavelet transform (PWT) features, Tree-structured Wavelet Transform (TWT) features and multiresolution simultaneous autoregressive model (MR-SAR) features.

Basically, Gabor filters are a group of wavelets, with each wavelet capturing energy at a specific frequency and a specific direction. Expanding a signal using this basis provides a localized frequency description, therefore capturing local features/energy of the signal. Texture features can then be extracted from this group of energy distributions. The scale (frequency) and orientation tunable property of Gabor filter makes it especially useful for texture analysis. Gabor Elementary Functions are Gaussians modulated by complex sinusoids. In two dimensions they are represented by

$$g(x,y) = \left(\frac{1}{2\pi\sigma_x\sigma_y}\right) e^{\left[\frac{-1}{2}\left(\frac{x^2}{{\sigma_x}^2}+\frac{y^2}{{\sigma_y}^2}\right)+2\pi jWx\right]} \quad (4)$$

The Fourier transform of g(x; y) is
$H(u,v)$

$$= e^{\left[\frac{-1}{2}\left(\frac{(u-w)^2}{{\sigma_u}^2}+\frac{v^2}{{\sigma_v}^2}\right)\right]} \quad (5)$$

where $\sigma_u = \frac{1}{2\pi\sigma_x}$ and $\sigma_v = \frac{1}{2\pi\sigma_y}$

A class of self-similar functions, referred to as the Gabor wavelets, is now considered. Let g(x; y) be the mother wavelet. Then a self-similar filter dictionary can be obtained by appropriate dilations and translations of g(x,y) through the generation function
$g_{mn}(x,y)$

$$= a^{-m}\ g(x', y') \quad (6)$$

where a > 1, m; n =integer.

$$x' = a^{-m}(x\cos\theta + y\sin\theta)$$

$$y' = a^{-m}(y\cos\theta - x\sin\theta)$$

where $\theta = \frac{n\pi}{k}$ and K is the total number of orientations.

The scale factor a^{-m} in equation (6) ensures that the energy is independent of m

$$E_{mn} = \iint |g_{mn}|^2\, dxdx \quad (7)$$

The non-orthogonality of Gabor wavelets implies that there is redundant information in the filtered images, and the following strategy is used to reduce this redundancy.

The design strategy is to ensure that the half peak magnitude cross-sections of the filter reponses in the frequency spectrum touch each other. This results in the following formulas for computing the filter parameters σ_u and σ_v

$$a = \left(\frac{U_h}{U_L}\right)^{\frac{1}{S-1}} \quad (8)$$

$$\sigma_u = \frac{(a-1)U_h}{(a+1)\sqrt{2\ln(2)}} \quad (9)$$

$$\sigma_v = \tan\left(\frac{\pi}{2k}\right)\left[U_h - 2\ln(2)\left(\frac{{\sigma_u}^2}{U_h}\right)\right][2\ln 2 - (\frac{(2\ln(2))^2\,\sigma_u}{{U_h}^2})] \quad (10)$$

where

$$W = U_h, \theta = \frac{\pi}{k}, m = 0,1,\dots,S-1.$$

Here m is scale. In order to eliminate sensitivity of the filter response to absolute intensity values, the real (even) components of the 2-D Gabor filters are biased by adding a constant to make them zero mean. Filtering the image I(x; y) with $g_{mn}(x, y)$ results in

$$W_{mn} = \int I(x,y)g^*_{mn}(x-x1, y - y1)dx1dy1 \quad (11)$$

where * indicates the complex conjugate.

2.2.3 Curvelet feature extraction

The digital Curvelet transform is taken on a 2-D Cartesian grid f[m,n], $0 \le m < M, 0 \le n < N$,

$$CT^D(a,b,\theta) = \sum_{\substack{0\le m<M \\ 0\le n<N}} f[m,n]\psi^D_{a,b,\theta}[m,n] \quad (12$$

Equation (12) is implemented in frequency domain and can be expressed as,

$$CT^D(a,b,\theta) = \text{IFFT}(\text{FFT}\left(f([m,n]) \times \text{FFT}\left(\psi^D_{a,b,\theta}[m,n]\right)\right) \quad (13)$$

After obtaining the coefficients in $CT^D(a,b,\theta)$, the mean and standard deviation are calculated from each set of Curvelet coefficients. Therefore, if p Curvelets are used for

the transform, 2p texture features are obtained. A 2p dimension texture feature vector is used to represent each image in the database for image retrieval. This feature extraction is applied to each of the images in the database. At the end, each image in the database is represented and indexed using its Curvelet feature vector.

2.3 Numerical image characterization: Signatures

The way the feature vectors are computed, based on the wavelets Gabor and Curvelet transform is described in this section II.2 (See Figure. 1). Here, some statistical measures are used to generate the feature vectors. More precisely, the mean μ_{mn} and the standard deviation σ_{mn} of the energy distribution of the multiresolution transform coefficients are used to capture the image information and, thus, to form the feature vector f:

$$\mu_{mn} = \iint |W_{mn}| dxdy \quad (14)$$

$$\sigma_{mn} = \sqrt{\iint |(W_{mn} - \mu_{mn})^2| dxdy} \quad (15)$$

For the Gabor Wavelet Transform, the values of $|W_{mn}|$ denote the energy distribution of the transform coefficients after convolving an image I with the Gabor wavelet g_{mn}. By considering a total number of S=4 scales and K = 6 orientations, the resulting feature vector is computed as follows:

$$f = [\mu_{11}, \sigma_{11}, \dots, \mu_{KS}, \sigma_{KS}] \quad (16)$$

For the Curvelet transform, let a Curvelet feature vector of a texture image be denoted by fc and the standard deviation and mean of the Curvelet subband at scale a and orientation θ are denoted $\sigma_{a\theta}$ and $\mu_{a\theta}$ respectively.

Images are decomposed using 4 levels Curvelet transform. Based on the subband division, with 4 levels analysis, 50 (=1+16+32+1) subbands of Curvelet coefficients are computed. However, Curvelet at angle θ produces the same coefficients as Curvelet at angle $\theta + \pi$. Therefore, half of the subbands at scale 2 and 3 are discarded due to this symmetry. As the result, 26 (=1+8+16+1) subbands are preserved, and a 52 dimension feature vector is generated for each image in the database. Then the Curvelet feature vector fc can be expressed as [24]

$$fc = [\mu_{11}, .., \mu_{1J}, \dots, \mu_{I1}, \dots, \mu_{IJ}, \sigma_{11}, .., \sigma_{1J}, \dots, \sigma_{I1}, \dots, \sigma_{IJ}] \quad (17)$$

Where, I is the finest scale and J is the total number of subbands taken at scale a. This feature vector is then used to index the image in the feature database.

2.4 Measure for similarity retrieval

The texture similarity measurement of a query image Q and a target image T in the database is defined by: The effective feature distance obtained from the weighted sum of each feature distance component. It is given by:

$$D(Q,T) = \sqrt{\sum_{i=1}^{2p+2mn} (Q_i - T_i)^2} \quad (18)$$

Where

$$Q_i = [\alpha 1 * fc^q, \ \alpha 2 * f^q] \text{ and } T = [\alpha 1 * fc^t, \ \alpha 2 * f^t]$$

Where Q_i is the feature vector of query image extracted from the BIMF1 + BIMF2 component using Curvelet Transform and Gabor Wavelet, T_i is the feature vector of target image extracted from the residue after IMF1 + IMF2 component using Curvelet Transform and Gabor wavelets.

$\alpha 1$ is the weight of the first component, and $\alpha 2$ is the weight of the second component.

3. Experiment results and retrieval performance

In order to evaluate the performance of the proposed scheme, we used the same texture database, which was used by Do and Vetterli[25]. These images are classified into 13 texture classes as shown in Figure 6, each texture of size 512×512. From these images non-rotated image database is created by dividing each 0° version of the original textures into 16 disjoint regions with the same pixel size 128×128. We construct also rotated image database by taking four non-overlapping 128×128 subimages each from the original images at 0°, 30°, 60° and 120°. Both database sets contain 208 images each. The non-rotated set serves as the ideal case, where all images in the same class have the same orientation, for the rotated set. A comprehensive study, using several approach, is conducted on different databases. Table 2 shows the comparison of performances in percentage of retrieving relevant image for the non-rotated and the rotated set. In the first experiment, non-rotated database is used. The result of proposed method is compared with standard DWT (with normalized Euclidean distance as similarity measure) and the vector wavelet domain HMM (WD_HMM) as reported in [25] and the

rotation invariant texture features using rotated complex wavelet as reported in [26].

In the second series of experiments, we have tested the rotation invariant property of proposed method. In this experiment we used rotated database set. Results have been compared with the isotropic rotationally invariant features extracted from DWT developed by Porter [27] and rotation invariant property obtained with the vector steerable WD_HMM as reported in [25] and the rotation invariant texture features using rotated complex wavelet as reported in [26]. Experimental results from Table 2 and table 3 show that on both the databases the proposed method outperforms the other existing methods.

In order to evaluate the quality of the images retrieval approach, they should be compared with both Curvelet transform [24] and Gabor wavelets [7] applied directly on the original image. The performance of each retrieval method is estimated by comparing the fused images in terms of precision and recall. Performance of our system is studied by using each image in the database as the query image and top 30 similar images are retrieved by Euclidean distance based exhaustive search. Figure 7 shows the comparison between the retrieval performance of our method and Curvelet features and Gabor wavelet.

In our experience, the weight are $\alpha 1 = 0.8,\ \alpha 2 = 0.2$.

Table 2 : Retrieval accuracy(*Rotated database set***)**

Texture Name	*Rotated database set*			
	DWT	*SWD_ HMM*	*DTC WT+ DTRC WF*	*Proposed Method*
Bark	93.75	88.67	100.0	92.91
Brick	56.25	75.47	81.25	88.43
Bubbles	75.00	65.00	87.50	99.37
Grass	100.0	100.0	100.0	98.54
Leather	75.00	100.0	87.50	99.06
Pigskin	75.00	87.73	93.75	88.75
Raffia	87.50	76.88	100.0	100
Sand	100.0	85.84	100.0	96.97
Straw	62.50	98.00	68.75	85.52
Water	100.0	84.90	100.0	99.89
Weave	100.0	99.00	100.0	100
Wood	56.25	89.62	68.75	96.25
Wool	87.50	80.00	93.75	82.81
AVG	82.21%	86.77%	90. 86%	94.50%

Table3: Retrieval accuracy (*Non-rotated database set***)**

Texture Name	*Non-rotated database set*			
	DWT	*SWD_ HMM*	*DTC WT+ DTR CWF*	*Proposed Method*
Bark	100.0	68.86	81.25	91.25
Brick	56.25	89.62	81.25	89.17
Bubbles	100.0	65.09	100.0	100
Grass	68.75	100.0	81.25	99.17
Leather	93.75	97.16	100.0	100
Pigskin	93.75	82.20	93.75	95.83
Raffia	75.00	68.86	100.0	100
Sand	87.50	88.67	100.0	98.33
Straw	43.75	87.73	87.50	81.67
Water	100.0	83.96	93.75	100
Weave	100.0	97.16	100.0	100
Wood	100.0	93.39	100.0	77.92
Wool	100.0	99.00	93.75	90.83
AVG	83.17%	86.41%	93.71%	94.16%

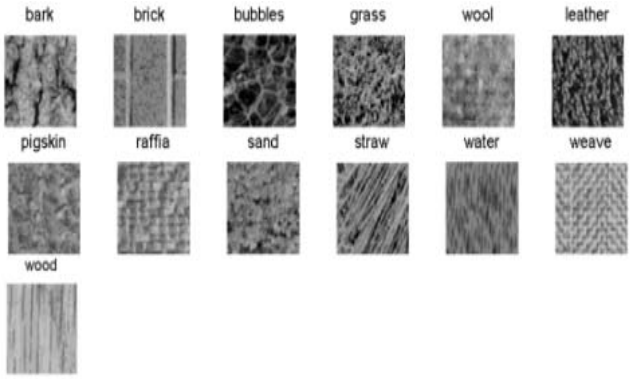

Fig. 6: The Brodatz texture data set from the USC-SIPI Images Database [28].

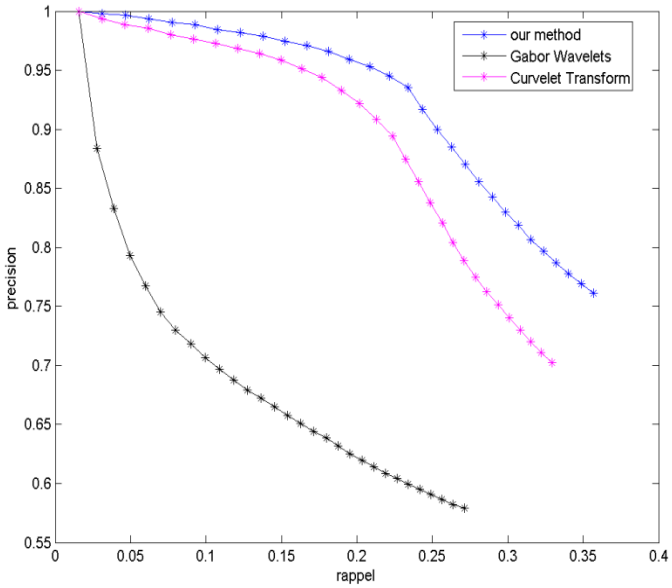

Fig.7: Average retrieval result of 832 queries ($\alpha 1 = 0.8$, $\alpha 2 = 0.2$)

4. Conclusions

In this paper we used the FABEMD, to obtain characteristic signatures of images, in the context of CBIR. It consists to split image into two components. On the first component, we apply the Curvelet transform while on the second component; we apply the Gabor filters and then compute the low order statistic from the transformed images. The extracted image features were then used to measure the similarity between images. To check the retrieval performance, texture database of 832 textures was created from Brodatz album. Our approach was evaluated and the result indicates that the proposed decomposition lead a strong potential towards the improvement of the performance.

References

[1]. C. T. Zahn and R. Z. Roskies. Fourier descriptors for plane closed curves. IEEE Transactions on Computer, C-21, No.1:269-281, 1972.

[2]. S.A.Dudani, K.J.Breeding,and R.B.McGhee. Aircraft identi cation by moment invariants. IEEE Transaction Computer, C26:39-45, January 1977.

[3]. A. P. Berman and L. G. Shapiro. A exible image database system for content-based retrieval. Computer Vision and Image Understanding, 75:175-195, 1999.

[4]. Z. N. Li, D. R. Zaiane, and Z. Tauber. Illumination invarit rieval. Journal of Visual Communication and Image Representation, 10(3):219-244, 1999.

[5]. TB. Serge, Greenspan, Hayit, Malik, Jitendra, and Puzicha. Shape matching and object recognition using shape contexts. IEEE Transactions on Pattern Analysis and Machine Intelligence, 24(4):509-522, 2002

[6]. R. M. HARALICK, K. SHANMUGAM et I. DINSTEIN. Textural features for image classification. IEEE Transactions on Systems, Man, and Cybernetics, SMC-3(6):610–621, nov 1973.

[7]. B. S. Manjunath and W. Y. Ma. Texture features for browsing and retrieval of image data. IEEE Trans. on PAMI, 18:837-842, 1996.

[8]. L. M. Kaplan. Fast texture database retrieval using extended fractal features. SPIE 3312, SRIVD VI:162-173, 1998.

[9]. G. Cross, A. Jain. Markov random field texture models. IEEE Transactions on Pattern Analysis and Machine Intelligence 5 (1):25-39, 1983.

[10]. J. Mao, A. Jain. Texture classification and segmentation using multiresolution simultaneous autoregressive models. Pattern Recognition 25 (2): 173-188, 1992.

[11]. JF. Liu, R. Picard. Periodicity, directionality, and randomness: Wold features for image modeling and retrieval. IEEE Transactions on Pattern Analysis and Machine Intelligence 18 (7): 722-733, 1996.

[12]. Zegarra, J. A. M., Leite, N. J., and Torres, R. D. S. Wavelet-based fingerprint image retrieval. Journal of computational and applied mathematics 277, 2 (2009), 294–307.

[13]. H. J. Bae and S. H. Jung, “Image Retrieval Using Texture Based on DCT,” Proc. of Int. Conf. on Information, Communications and Signal Processing, Singapore, pp. 1065-1068, 1997.

[14]. J. Starck, E. J. Candès, and D. L. Donoho, The Curvelet Transform for Image Denoising, IEEE Transactions on Image Processing, 11(6):670- 684, 2002.

[15]. Minh N. Do, Directional Multiresolution Image Representations, PhD Thesis, EPFL, 2001.

[16]. Bhuiyan, S.M.A, Adhami, R.R. Khan, J.F, “A novel approach of fast and adaptive bidimensional empirical mode decomposition” March 31 2008-April 4 2008 ICASSP 2008. IEEE International Conference.

[17]. J. C. Nunes, Y. Bouaoune, E. Delechelle, O. Niang, Ph. Bunràel, “Image analysis by bidimensional empirical mode decomposition,” Image and Vision Computing, Vol. 21 pp. 1019–1026, 2003.

[18]. Huang and al, "The empirical mode decomposiion and Hilbert spectrum for non linear and non-stationary time series analysis," Proc. Roy. Soc. London A, Vol. 454, pp. 903-995, 1998.

[19]. C. Damerval, S. Meignen, V. Perrier, “A fast algorithm for bidimensional EMD,” IEEE Signal

Processing Letters, Vol. 12, No. 10, pp. 701-704, 2005.

[20]. B. Huan, Q. Xie, S. Peng, "EMD sifting based on bandwidth," IEEE Signal Processing Letters, Vol. 14, No. 8, pp. 537-540, 2007.

[21]. S.Jai-Andaloussi, M. Lamard, G. Cazuguel, H. Tairi, M. Meknassi, C. Roux, B. Cochener, Content Based Medical Image Retrieval Based on BEMD: use of Generalized Gaussian Density to model BIMFs coefficients, International Journal on Graphics, Vision and Image Processing, Vol 10, Issue 2, June 2010.

[22]. E. Candes et al, Fast Discrete Curvelet Transforms, Multiscale Modeling and Simulation, 5(3): 861-899, 2006.

[23]. G.V. de Wouwer, P. Scheunders, D.V. Dyck Statistical texture characterization from discrete wavelet representations. IEEE Transactions on Image Processing 8 (4) 592-598, 1999.

[24]. I. Sumana, M. Islam, D. S. Zhang and G. Lu, "Content Based Image Retrieval Using Curvelet Transform," a camera ready presentation In Proc. Of IEEE International Workshop on Multimedia Signal Processing (MMSP08), Cairns, Queensland, Australia, ISBN 978-1-4244-2295-1, pp.11-16, October 8-10, 2008.

[25]. M. N. Do and M. Vetterli, Rotation Invariant Texture Characterization and Retrieval using Steerable Wavelet-Domain Hidden Markov Models, IEEE Trans. on Multimedia, pp. 517-527, Dec. 2002.

[26]. Manesh Kokare, P. K. Biswas and B. N. Chatterji, Rotation invariant texture features using rotated complex wavelet for content based image retrieval, International Conference on Image Processing, Singapore , 2004, pp 393-396.

[27]. R. Porter and N. Canagajah, Robust Rotation Invariant Texture Classification: Wavelet, Gabor filter and GMRF based Schemes, IEE Proc. Vis. Image Signal Processing, Vol. 144 (3), June 1997, pp. 180-188.

[28]. The USC-SIPI Image Database. http://sipi.usc.edu/database/.

Mohamed El Hacen Ould Mohamed Dyla, received his Master's degree in 2008 from faculty of sciences, Fez Morocco. He is pursuing his PhD degree at the laboratory of computer, imaging and numerical analysis. His main research interests are; images decomposition, image retrieval and video retrieval.

Hamid Tairi received his PhD degree in 2001 from the University Sidi Mohamed Ben Abdellah, Morocco. In 2002 he has done a postdoc in the Image Processing Group of the Laboratory LE2I (Laboratoire d'Electronique, Informatique et Image) in France. Since 2003, he has been a professor at the University Sidi Mohamed Ben Abdellah, Morocco. His research interests are in visual tracking for robotic control, in 3-D reconstruction, in medical image, in visual information retrieval and pattern recognition.